Electronic Supplementary Material (ESI) for CrystEngComm.
This journal is © The Royal Society of Chemistry 2020

Supporting Information

Fluorination as a route towards unlocking the hydrogen bond donor ability of phenolic compounds in self-assembled monolayers

Harry Pinfold,[1] Graham Pattison‡[1] and Giovanni Costantini[1]

1) Department of Chemistry, University of Warwick, Gibbet Hill Road, Coventry, CV4 7AL, UK.

‡) Present address: Chemistry Research Group, School of Pharmacy and Biomolecular Sciences, University of Brighton, Brighton, BN2 4GJ, UK.

Contents:

1. Experimental details
2. Large-scale STM images of the multicomponent networks
3. Self-assembly behaviour of 3TPTZ and 4TPTZ
4. Attempts to fabricate multicomponent networks with HQ
5. Geometric considerations relating to the formation of O−H⋯N(pyridyl) hydrogen bonds
6. References

1. Experimental details

Commercially available TFHQ (Alfa Aesar, 96%), HQ (Acros Organics, 99.5%), 3TPTZ (Alfa Aesar, 97%) and heptanoic acid (Acros Organics, 98%) were used without further purification. 4TPTZ was prepared as follows:

A mixture of 4-cyanopyridine (1.0 g, 9.6 mmol), 18-crown-6 (0.1 g, 0.38 mmol) and potassium hydroxide (22.5 mg, 0.40 mmol) was dissolved in decalin (1.0 cm^3) and heated with stirring at 200 °C under nitrogen for 3 h. The solvent was evaporated under high vacuum to give a brown solid. This was washed with hot pyridine (3×5.0 cm^3) to leave white crystals, which were dissolved in 2.0 M hydrochloric acid (5.0 cm^3). Addition of aqueous ammonia led to the precipitation of a white solid which was filtered and dried under high vacuum; yield 0.65 g (65%). ^1H NMR (400 MHz, $CDCl_3$,) 8.56 (6 H, d, *J* = 5.6 Hz) and 8.94 (6 H, d, *J* = 5.6 Hz)

Solutions of 3TPTZ and TFHQ were prepared at a concentration of 10^{-2} M by dissolving each of the solid materials in heptanoic acid via sonication and gentle heating. 4TPTZ was somewhat less soluble than 3TPTZ, and even after extensive sonication we were not able to dissolve it at a concentration of 10^{-2} M. Therefore, saturated solutions of 4TPTZ were used. These were prepared by sonicating and gently heating an excess of solid 4TPTZ in heptanoic acid. These solutions were left to settle for at least 24 hours before the saturated 4TPTZ solution was separated from the remaining solid via filtration. The solutions used to prepare the networks described in the main text were prepared by mixing equal volumes of 10^{-2} M TFHQ solution with 10^{-2} M 3TPTZ/saturated 4TPTZ solution. Due to the high affinity of TFHQ for 4TPTZ, precipitation of what were presumably 3D cocrystals was observed to occur a few minutes after combining the two solutions. Solution decanted from these 3D cocrystals was deposited onto a HOPG substrate (TipsNano, ZYB), and the coassembly of 4TPTZ with TFHQ was observed at the interface between this solution and the HOPG surface. With 3TPTZ the situation was slightly different. 3D cocrystallisation of the two building blocks was again observed to occur; however, deposition of solution decanted from the 3D cocrystals only led to the formation of occasional, isolated domains of the 3TPTZ/TFHQ assembly. We expect that this is due to the 3D cocrystallisation significantly depleting the concentration of the molecules in solution. Luckily, the 3D cocrystallisation of 3TPTZ with TFHQ typically didn't start for several hours. By depositing freshly prepared solutions, i.e., before any 3D cocrystallisation had occurred, we observed essentially full surface coverage of the 3TPTZ/TFHQ bimolecular network. As it was far easier to study the assembly at high coverage, this is the method that was adopted. It should be noted that several hours after deposition, the bimolecular assembly was typically observed to disappear, and we would begin to see large regions of the surface on which no assembly was present and occasional domains of the hexagonal assembly of 3TPTZ described in section 3. These observations are consistent with a significant change in the composition of the deposited solution. After this had occurred, visual inspection of the sample's surface typically revealed that 3D cocrystals had precipitated from the solution. With both 3TPTZ and 4TPTZ we also attempted to use more dilute solutions to avoid 3D cocrystallisation. Solutions in which both 3TPTZ/4TPTZ and TFHQ were present at a concentration of 5×10^{-4} M were found to be stable, i.e., precipitation was not observed. With 3TPTZ, deposition of these more dilute solutions did not lead to the formation of any self-assembled structures. With 4TPTZ these more dilute solutions led to the formation of the same multicomponent assembly that was observed with the more concentrated solutions, i.e., those from which precipitation of 3D cocrystals had occurred.

All STM measurements were performed using a Veeco STM equipped with an A-type scanner head, coupled with a Nanoscope E controller. Measurements were recorded under ambient conditions. The temperature was typically within the range of 21 – 23°C. All images were recorded in constant current mode. The tunnelling parameters used for each of the presented images are given in the figure captions. In general, bias voltages (V_{bias}) in the range from −0.8 to −1.2 V and tunnelling currents (I_{set}) of 50 – 200 pA were found to be optimal for imaging the molecular overlayer. The bias voltage was applied to the sample. STM tips were prepared by mechanically cutting 80/20 Pt/Ir wire (Goodfellow). Prior to each experiment, HOPG substrates were freshly prepared by cleaving the upper layers using scotch tape. All STM images were processed and analysed using WsXM[1] and LMAPper[2]. All of the presented images were Gaussian filtered. In order to eliminate the effects of thermal drift such that accurate lattice parameters could be obtained, the underlying HOPG surface was used for calibration. Partway through recording an image of the molecular overlayer, the tunnelling conditions were adjusted such that the underlying atomic lattice of the HOPG surface could be imaged. Within the resultant images, both the molecular overlayer and the atomic lattice of the HOPG surface could be resolved. The images were then calibrated using the known lattice parameters of the HOPG surface (0.246 nm, hexagonal). The reported lattice parameters are the average values obtained from at least nine repeat experiments, and the reported uncertainties on these values represent the corresponding standard deviations. The high-resolution STM images presented in the main text were calibrated using these accurately determined lattice parameters to eliminate any effects of thermal drift.

2. Large-scale STM images of the multicomponent networks

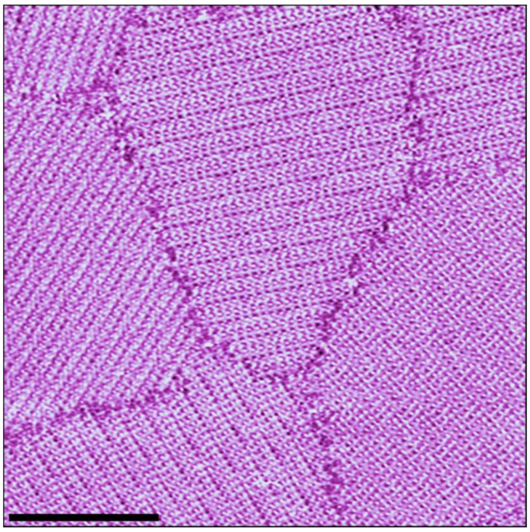

Fig. S1 Large-scale STM image showing the assembly formed via the codeposition of TFHQ and 3TPTZ at the heptanoic acid/HOPG interface. Tunnelling parameters: V_{bias} = −0.9 V, I_{set} = 50 pA. Scale bar = 20 nm.

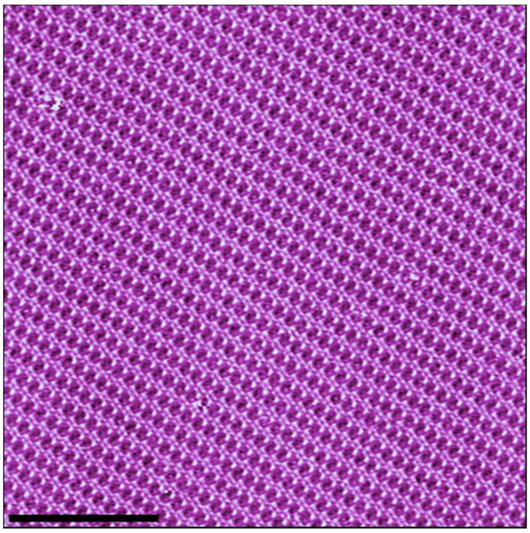

Fig. S2 Large-scale STM image showing the assembly formed via the codeposition of TFHQ and 4TPTZ at the heptanoic acid/HOPG interface. Tunnelling parameters: V_{bias} = −0.9 V, I_{set} = 100 pA. Scale bar = 20 nm.

3. Self-assembly behaviour of 3TPTZ and 4TPTZ

The self-assembly behaviour of 4TPTZ has previously been studied at the heptanoic acid/HOPG interface. Kampschulte et al. have reported that 4TPTZ does not self-assemble on its own;[3] however, Li et al. have reported that it does.[4] As we have previously reported,[5] our observations are consistent with those of Kampschulte et al., i.e., we never observed any indication that 4TPTZ self-assembles at the heptanoic acid/HOPG interface under ambient conditions.

We have also previously studied the self-assembly behaviour of 3TPTZ at the heptanoic acid/ HOPG interface. The results presented here are consistent with those that we have reported previously.[5] Deposition of a 10^{-2} M solution of 3TPTZ dissolved in heptanoic acid leads to the formation of a hexagonal assembly (see Fig. S3). Within this network, two equivalent lattice vectors, which have lengths of 3.5 ± 0.1 nm, are separated by an angle of 60 ± 3°. The individual 3TPTZ molecules can be clearly resolved in high-resolution STM images (see Fig. S4a). The 3TPTZ molecules are positioned such that they can interact with one another via C−H···N(pyridyl) interactions. Each 3TPTZ molecule interacts with two adjacent 3TPTZ molecules via these weak interactions. This results in the arrangement of the 3TPTZ molecules into cyclic structures, each of which is composed of six molecules. These cyclic structures are then further packed together on the surface into a hexagonal array. The pyridyl nitrogen atoms that do not engage in C−H···N(pyridyl) interactions, i.e., those on the periphery of the cyclic structures, are not positioned such that they can interact with adjacent 3TPTZ molecules. These free pyridyl nitrogen atoms are effective hydrogen bond acceptor sites and likely interact with coadsorbed solvent molecules via O−H···N(pyridyl) bonds. Such hydrogen bonds are expected to be fairly strong, and coadsorbed heptanoic acid molecules can be readily incorporated into the space between the cyclic structures. Although it cannot be clearly resolved, structure consistent with the presence of coadsorbed solvent molecules in the interstices between the cyclic structures can be seen in Fig. S4a. A tentatively proposed model is given in Fig. S4b.

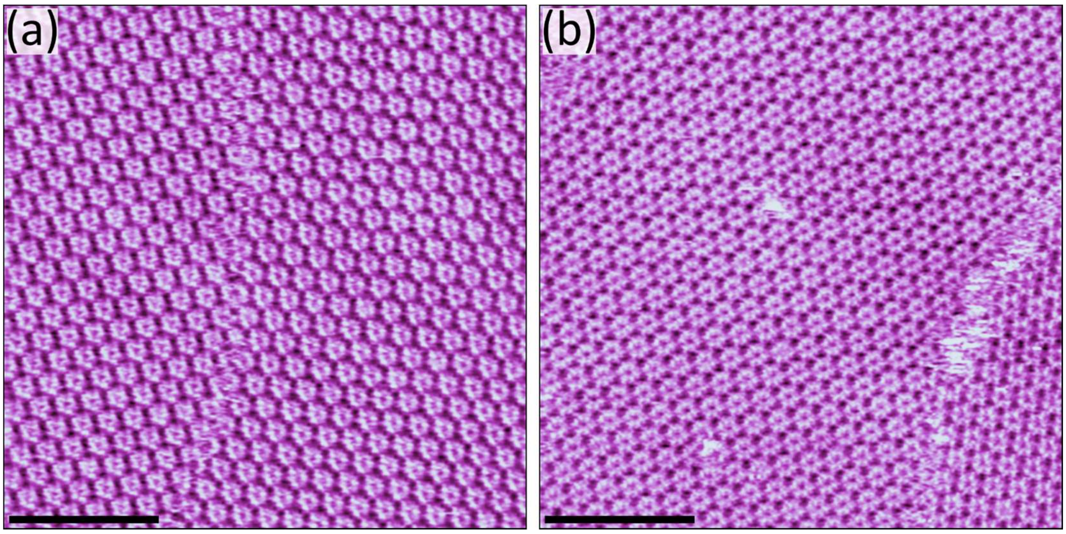

Fig. S3 Large-scale STM images showing the assembly of 3TPTZ at the heptanoic acid/HOPG interface. Tunnelling parameters: (a) V_{bias} = −0.9 V, I_{set} = 150 pA, (b) V_{bias} = −1.2 V, I_{set} = 200 pA. Both scale bars = 20 nm.

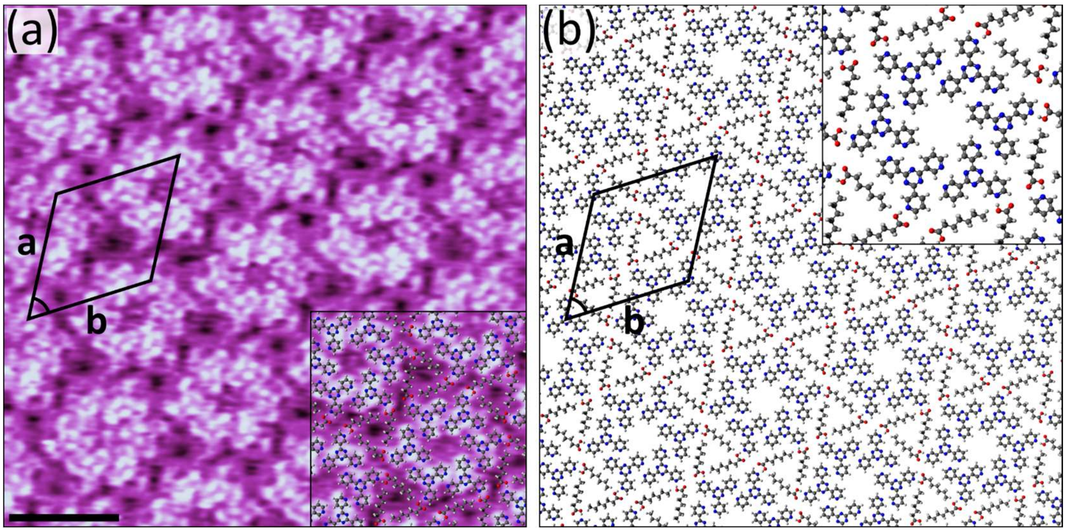

Fig. S4 (a) STM image showing the assembly of 3TPTZ with coadsorbed solvent molecules at the heptanoic acid/HOPG interface. Tunnelling parameters: V_{bias} = −0.9 V, I_{set} = 50 pA. Unit cell parameters: a = b = 3.5 ± 0.1 nm, angle 60 ± 3°. Scale bar = 3 nm. (b) Proposed model for the assembly.

We also investigated how the concentration of 3TPTZ in solution influences the assembly. We sampled solutions with concentrations in the range of 10^{-2} – 10^{-5} M. We did not observe any evidence of any concentration-dependent polymorphism. The assembly of 3TPTZ could be reliably observed covering essentially the entire surface of the sample at concentrations ranging from 10^{-2} M down to ~2.5×10^{-3} M. These results are summarised in Fig. S5.

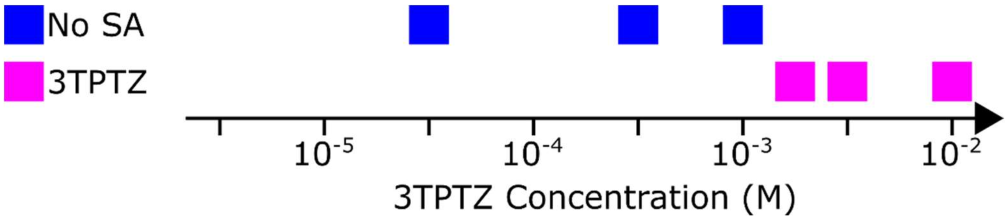

Fig. S5 Profile summarising the different observations made at the heptanoic acid/HOPG interface as the concentration of 3TPTZ in solution is changed. Blue squares indicate that no assembly could be observed, and pink squares indicate that the hexagonal assembly of 3TPTZ was observed.

4. Attempts to fabricate multicomponent networks with HQ

In order to try to form multicomponent networks with HQ and 3TPTZ/4TPTZ, we prepared mixed solutions and used STM to investigate the interface between these solutions and the HOPG surface. The experiments were conducted in exactly the same manner as those conducted with TFHQ. A range of different solution compositions were tested as the formation of multicomponent networks may strongly depend on the composition of the solution. Unlike with TFHQ, 3D cocrystals of HQ and 3TPTZ/4TPTZ were not observed to precipitate from solution. For every solution composition tested, at least five distinct ~0.5 μm^2 regions of the interface between the solution and a freshly prepared HOPG sample were surveyed via STM.

3TPTZ

Deposition of solutions containing both HQ and 3TPTZ at 5×10^{-3} M—the same concentration that was successfully used with TFHQ—did not lead to the coassembly of 3TPTZ with HQ. Instead, all that could be observed was the hexagonal assembly formed when only 3TPTZ is present in solution. Reduction of the concentration of 3TPTZ is expected to disfavour the formation of this hexagonal assembly and therefore increase the likelihood of coassembly with HQ. However, even when the concentration of 3TPTZ was reduced such that the hexagonal assembly was no longer present, we simply observed the absence of any assembly rather than the coassembly of 3TPTZ with HQ. The results from the different solution compositions tested are summarised in Fig. S6. As can be seen by comparison of Fig. S5 with Fig. S6, the presence of HQ in the solution at a relatively high concentration of 5×10^{-3} M does nothing to disrupt the self-assembly behaviour of 3TPTZ. The system behaves as if HQ was simply not present.

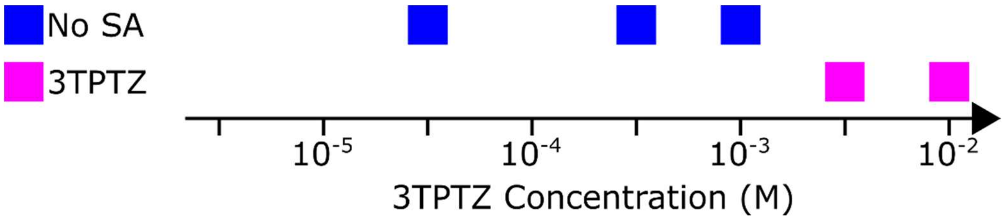

Fig. S6 Profile summarising the different observations made at the heptanoic acid/HOPG interface as the concentration of 3TPTZ is adjusted in a solution containing HQ at a concentration of 5×10^{-3} M. Blue squares indicate that no assembly could be observed, and pink squares indicate that the hexagonal assembly of 3TPTZ was observed.

4TPTZ

Deposition of solutions containing HQ and 4TPTZ yielded analogous results to those obtained with 3TPTZ. Mixed solutions in which the concentration of HQ was 5×10^{-3} M and the concentration of 4TPTZ was 0.5 × saturated did not lead to the formation of any coassembled structures. Note that this solution composition is similar to that which was successful with TFHQ, although the effective concentrations of both components in the 4TPTZ/TFHQ solutions are actually slightly lower due to the precipitation of 3D cocrystals. We also tested solutions in which both HQ and 4TPTZ were present at concentrations of 5×10^{-4} M as this composition was also successful with TFHQ. With HQ we observed no evidence of the formation of any assembly.

A range of different solution compositions in which the relative molar ratios of the two components were varied were also tested. These different solution compositions are summarised in Fig. S7. We did not observe any indication of the formation of any self-assembled structures under any of the tested conditions.

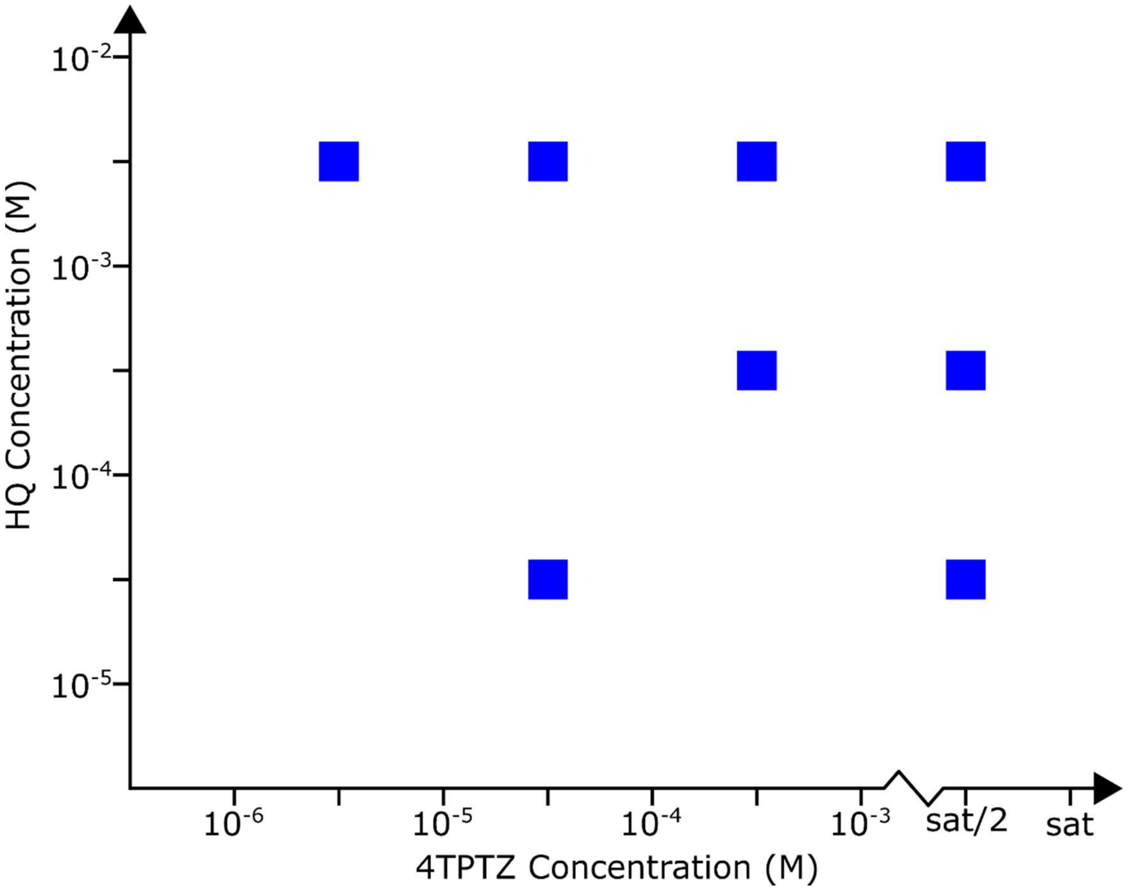

Fig. S7 Profile summarising the observations made at the heptanoic acid/HOPG interface for solutions containing both 4TPTZ and HQ at a range of different concentrations. Blue squares indicate that no assembly could be observed.

5. Geometric considerations relating to the formation of O−H···N(pyridyl) hydrogen bonds

A schematic illustration of the possible O−H···N(pyridyl) hydrogen bonding interaction between HQ and a pyridyl group is shown in Fig. S8. The molecules are positioned coplanar to one another as flat molecules such as these typically adsorb with the plane of their aromatic rings parallel to the underlying surface. The optimal hydrogen bonding geometry typically occurs when the hydrogen bond adopts a linear geometry[6,7] and when the position of the partaking hydrogen atom is aligned with the projection of a lone pair of the acceptor atom[6,8], i.e., when the angles θ_1 and θ_2 in Fig. S8 both have values of 180°. Within three-dimensions, the molecules are not restricted to being coplanar; therefore, the optimal hydrogen bonding geometry can be achieved. However, upon surface confinement, flat molecules are typically restricted to approximately coplanar configurations. As has previously been studied theoretically,[9] enforcement of such a coplanar arrangement disrupts the ideal hydrogen bonding geometry between phenols and pyridyl groups due to the steric interaction between the hydrogen atoms (H_a and H_b in Fig. S8) attached to the aromatic rings. Although hydrogen bonds do have significant flexibility, deviation from the ideal linear arrangement is associated with a reduction in hydrogen bond strength.[7,8] This could potentially be a significant factor in the scarcity of examples of monolayer systems based on hydrogen bonding interactions between phenolic and pyridyl groups. As is mentioned in the main text, the aromatic carboxylic acid TPA, which is not structurally dissimilar from HQ, does coassemble with 4TPTZ via O−H···N(pyridyl) hydrogen bonds into an ordered monolayer at the heptanoic acid/HOPG interface.[3] It is worth noting that, even when restricted to coplanar arrangements, TPA clearly seems to be less sterically hindered towards the formation of optimal linear hydrogen bonds than HQ.

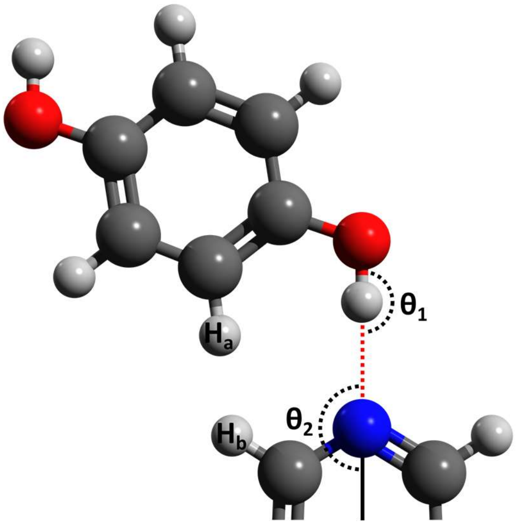

Fig. S8 Schematic illustrating the potential O−H···N(pyridyl) hydrogen bond that could occur between HQ and 3TPTZ/4TPTZ when the two molecules are confined to a coplanar arrangement. The hydrogen bond is represented by a red dashed line. The solid black line represents the axis centralised on the direction of the pyridyl nitrogen atom's lone pair of electrons.

The geometric restrictions on analogous systems formed with TFHQ is less clear. The hydrogen atom H_a in the HQ molecule in Fig. S8 is substituted for a fluorine atom in TFHQ. This fluorine atom can likely interact somewhat favourably with H_b via a weak C−H···F interaction. Although there may be an attractive interaction between this fluorine atom and H_b, these two atoms would have to be extremely close together for an O−H···N(pyridyl) hydrogen bond of reasonable length to occur with its optimal linear geometry. Therefore, we suspect that there is likely still a significant steric interaction that prevents an O−H···N(pyridyl) hydrogen bond with optimal linear geometry being formed with TFHQ. Although STM images certainly cannot be used to obtain precise atomic positions, it is clear from the proposed models given in the main text that the O−H···N(pyridyl) hydrogen bonds between TFHQ and 3TPTZ/4TPTZ do not adopt an optimal linear geometry.

6. References

1 I. Horcas, R. Fernández, J. M. Gómez-Rodríguez, J. Colchero, J. Gómez-Herrero and A. M. Baro, *Rev. Sci. Instrum.*, 2007, **78**, 013705.

2 LMAPper - The SPM and Mol Viewer, https://sourceforge.net/projects/spm-and-mol-viewer/, (accessed August 1, 2019).

3 L. Kampschulte, S. Griessl, W. M. Heckl and M. Lackinger, *J. Phys. Chem. B*, 2005, **109**, 14074–14078.

4 M. Li, P. Xie, K. Deng, Y.-L. Yang, S.-B. Lei, Z.-Q. Wei, Q.-D. Zeng and C. Wang, *Phys. Chem. Chem. Phys.*, 2014, **16**, 8778–8782.

5 H. Pinfold, C. Greenland, G. Pattison and G. Costantini, *Chem. Commun.*, 2020, **56**, 125–128.

6 T. Steiner, *Angew. Chem. Int. Ed.*, 2002, **41**, 48–76.

7 P. A. Wood, F. H. Allen and E. Pidcock, *CrystEngComm*, 2009, **11**, 1563.

8 A. L. Llamas-Saiz, C. Foces-Foces, O. Mo, M. Yañez and J. Elguero, *Acta Crystallogr. Sect. B*, 1992, **48**, 700–713.

9 S. G. W. Ginn, *J. Mol. Struct.*, 1978, **49**, 137–153.